ELSEVIER

Chemical Geology 193 (2003) 59–80

CHEMICAL GEOLOGY
INCLUDING
ISOTOPE GEOSCIENCE

www.elsevier.com/locate/chemgeo

Calculation of oxygen isotope fractionation in magmatic rocks

Zi-Fu Zhao, Yong-Fei Zheng*

School of Earth and Space Sciences, University of Science and Technology of China, Hefei 230026, PR China

Received 12 June 2001; accepted 26 July 2002

Abstract

The increment method is applied to calculation of oxygen isotope fractionation factors for common magmatic rocks. The ^{18}O-enrichment degree of the different compositions of magmatic rocks is evaluated by the oxygen isotope indices of both CIPW normative minerals and normalized chemical composition. The consistent results are obtained from the two approaches, pointing to negligible oxygen isotope fractionation between rock and melt of the same compositions. The present calculations verify the following sequence of ^{18}O-enrichment in the magmatic rocks: felsic rocks>intermediate rocks>mafic rocks> ultramafic rocks. Two sets of internally consistent fractionation factors are acquired for phenocryst–lava systems at the temperatures above 1000 K and rock–water systems in the temperatures range of 0–1200 °C, respectively. The present calculations are consistent with existing data from experiments and/or empirical calibrations. The obtained results can be used to quantitatively determine the history of water–rock interaction and to serve geological thermometry for various types of magmatic rocks (especially extrusive rocks).

Keywords: Fractionation factor; Oxygen isotope; Theoretical calculation; Chemical composition; Magmatic rock

1. Introduction

Magmatic rocks are one of the most important components in both continental and oceanic crusts. Oxygen isotopes have been widely used in conjunction with other geochemical and petrological information to identify geologically favorable situations that illustrate important magmatic phenomena including the generation, evolution, and crystallization of magma (e.g., Taylor and Sheppard, 1986; Eiler, 2001). For example, oxygen isotope studies can play an important role in determining the origin of aqueous fluids involved in the formation of felsic magmas because fluid–rock interaction effects are most clear-cut when low-$\delta^{18}O$ surface water is involved in the isotopic exchange and melting processes (Taylor, 1971, 1974, 1988). In order to interpret various oxygen isotope data for magmatic rocks, the processes such as Rayleigh fractionation and equilibrium crystallization of magmas, subsolidus interaction between magmatic rocks and water must be taken into account. The magnitudes of oxygen isotope effects important for studies of fluid–rock interaction and melt–mineral fractionation are generally much larger than uncertainties in the reduced partition function ratios of minerals and melts. These demand good estimates of fractionation factors

* Corresponding author. Fax: +86-551-3603554.
E-mail address: yfzheng@ustc.edu.cn (Y.-F. Zheng).

0009-2541/02/$ - see front matter © 2002 Elsevier Science B.V. All rights reserved.
PII: S0009-2541(02)00226-7

of oxygen isotope in melt–mineral, melt–vapor or whole-rock–mineral systems.

A number of recent studies, based on phenocryst data by laser fluorination technique, have revealed considerable variations in the oxygen isotope composition of mantle-derived magmas and significant fractionations between phenocryst and lava (e.g., Eiler et al., 1995, 1996a,b, 1997, 2000; Baldridge et al., 1996; Macpherson and Mattey, 1997; Harris et al., 2000). It appears that oxygen isotope fractionations between phenocryst and lava cannot be neglected and that the isotopic fractionation behavior of mantle-derived rocks may differ from that of their original magmas. Despite their critical importance in interpreting oxygen isotope data for magmatic rocks, little attention has been paid to calibration of oxygen isotope fractionation between magmatic rocks and water and between phenocryst and lava.

Kalamarides (1986) empirically estimated oxygen isotope fractionations between phenocryst (such as feldspar, clinopyroxene, olivine, Fe–Ti oxides with 50% magnetite and 50% ilmenite) and basaltic matrix (tholeiite at 1200–1550 K, and basalt at 1443 K) by employing the $\delta^{18}O$ values of whole-rocks and minerals from Kiglapait intrusion. Cole et al. (1987, 1992) experimentally determined oxygen isotope fractionations between altered basalt and water at 300–500 °C and between altered granitic gneiss, biotite quartz monzonite and water at 170–300 °C, respectively.

There have been a number of experimental calibrations of oxygen isotope fractionation involving molten and glassy silicates by exchange with CO_2. These include basaltic melt (Muehlenbachs and Kushiro, 1974), rhyolitic glass and melt (Palin et al., 1996), silica glass (Stolper and Epstein, 1991), albitic glass and melt (Matthews et al., 1994), anorthitic glass and melt (Matthews et al., 1998), and Na-melilite melt (Appora et al., 2000). These experiments were carried out by bracketing the equilibrium fractionation between two phases from both directions. The results suggest a general similarity between isotopic fractionations involving experimental melts and those involving minerals with similar cation chemistry. This similarity was used as the basis for models of fractionation involving melt compositions that have not yet been examined experimentally (e.g., Matthews et al., 1998). These models are generally indistinguishable from the assumption that silicate melts have reduced partition function ratios equal to the weighted sum of those for their normative mineral constituents. This assumption involves a translation of melt chemistry that was extended to calculations of mineral–melt fractionation factors by means of a simple "chemical-bond index" after Garlick (1966).

The studies of Taylor and Epstein (1962) on magmatic and metamorphic rocks showed that oxygen isotope fractionation in silicate minerals can be semi-quantitatively understood in terms of linear combinations of the various bond-types (Si–O–Si, Si–O–Al, and Si–O–M) present in each silicate structure. Garlick (1966) presented a chemical-bond index to outline the effect of chemical composition variation on oxygen isotope fractionation in high-temperature rocks. The use of the Garlick index in a procedure for predicting the temperature dependence of oxygen isotope fractionations was suggested by Schliestedt and Matthews (1987) and refined by Ganor et al. (1994). Palin et al. (1996) demonstrated that a summation of the oxygen isotope partitioning behavior of normative major minerals for silica and albitic glasses could be sufficient to describe that of rhyolitic melt. This implies that magmatic melts can generally exhibit fractionation behaviors similar to their chemically identical crystalline phase. However, the concept used by Garlick (1966) is simply based on the proportions of silicon and aluminum equivalents in the silicate phases, regardless of their structure. It is not sufficient to describe the quantitative relationship of oxygen isotope partitioning to rock chemical compositions containing various cations.

At the temperatures of melting and crystallization, melt/residue and crystal/magma fractionation factors may be greater than a few tenths of a permil and thus are not negligible in petrogenetic and geothermometric studies. With the increase in oxygen isotope data for phenocrysts and lavas, a systematical calculation of oxygen isotope fractionation in the magmatic rocks of different compositions is highly demanded for the purpose of quantitatively studying phenocryst–lava fractionations and fluid–rock interactions. Different from mineral, there is no simple crystal structure for magmatic rocks. Thus, it is impossible to theoretically calculate oxygen isotope fractionation in magmatic rocks by statistical mechanical methods. Nevertheless, the increment method modified by Zheng (1991, 1993a,b) for calculation of oxygen isotope fractiona-

tion factors between minerals and between minerals and water is capable of predicting oxygen isotope fractionation in magmatic rocks. This paper presents such a prediction that provides a first approximation to oxygen isotope fractionation factors for the magmatic rocks of different compositions.

2. Calculation method

The increment method has been an efficient means for calculating oxygen isotopic fractionation in solid minerals as a function of statistico-mechanical and crystal structural effects. This method was primarily developed by Schütze (1980) and modified by Zheng (1991, 1993a,b). It focuses on individual bonds, the relative strengths of which are given by integral ionic charges and bond-lengths determined from ionic radii. Cation mass is included in a form appropriate for diatomic molecules. Because the effects of both bond strength and cation mass on isotopic substitution have been taken into account, oxygen isotope fractionation in minerals is calculated as it moves away in increments from a reference mineral. According to the principle of the increment method, the degree of ^{18}O-enrichment in a mineral can be quantified by the oxygen isotope index (I-^{18}O) of the mineral relative to that of a reference mineral.

Using the modified increment method, oxygen isotope fractionation in metal oxide and hydroxides, wolframate, silicate, phosphate, carbonate, and sulfate minerals has been calculated systematically (Zheng, 1991, 1992, 1993a,b, 1995, 1996, 1997, 1998, 1999a). The validity of the theoretical calibrations at both high and low temperatures has been verified by existing data derived from: (1) isotope exchange experiments under hydrothermal or anhydrous (i.e., using carbonate as exchange medium) conditions (e.g., Zheng, 1991, 1993a,b, 1997, 1999a,b; Zhang et al., 1994; Rosenbaum and Mattey, 1995), (2) synthesis experiments at low temperatures (e.g., the rutile–water system: Bird et al., 1993; the brucite–water system: Xu and Zheng, 1998; aragonite–water and witherite–water systems: Zhou and Zheng, 2002), (3) theoretical calculations by statistico-mechanical methods (e.g., for magnetite and garnet: Becker and Clayton, 1976 in Zheng, 1995; Rosenbaum and Mattey, 1995) or using Moessbauer spectroscopic data (e.g., for hematite: Polyakov and Mineev, 2000), and (4) empirical estimates on the basis of natural data (e.g., apatites: Zheng, 1996). Application of the calculated fractionation factors to isotopic geothermometry has been illustrated for metamorphic rocks (Zheng et al., 1998, 1999, 2001, 2002; Fu et al., 1999; Xiao et al., 2002). These successes are encouraging for the extension of such calculations to the systems involving magmatic rocks.

In principle, the greater the I-^{18}O index of a mineral, the richer in ^{18}O the mineral. A magmatic rock is composed of either crystal minerals or silicate glass, and thus the I-^{18}O index of the magmatic rock depends primarily on the proportion of mineral assemblages or chemical composition. I-^{18}O indices of the common magmatic rocks can thus be calculated in terms of either their chemical compositions or available I-^{18}O indices of silicates and oxides. As a result, oxygen isotope fractionation factors between magmatic rocks and water and between phenocryst and lava can be obtained. Chemical compositions of the common magmatic rocks used in this study are after Le Maitre (1976), as listed in Table 1. The procedures of calculating I-^{18}O indices and corresponding $10^3\ln\beta$ values have been outlined by Zheng (1996) in detail and thus are not repeated here.

2.1. Oxygen isotope indices (I-^{18}O)

In the first step, the I-^{18}O of a rock in question relative to a reference mineral must be calculated. For this purpose, the CIPW normative minerals and normalized chemical compositions of the common magmatic rocks are used, respectively. The CIPW normative minerals have taken into account both crystal structures and chemical compositions and thus are appropriate for intrusive rocks. This assumes that the oxygen isotope fractionation property of a crystalline igneous rock is simply the sum of the fractionations of the individual minerals times their mole fraction. However, there are both crystalline and non-crystalline phases in volcanic rocks. The normalized chemical composition that is independent of crystal structure may be more reasonable to the calculation of I-^{18}O indices for the volcanic rocks. It appears that these are two different approaches in the calculation of rock I-^{18}O indices. Quartz is used as the reference

Table 1
Chemical composition of common magmatic rocks (%) (after Le Maitre, 1976)

Rock	SiO_2	TiO_2	Al_2O_3	Fe_2O_3	FeO	MnO	MgO	CaO	Na_2O	K_2O	H_2O^+	H_2O^-	P_2O_5	CO_2	Total
Nepheline syenite	54.99	0.60	20.96	2.25	2.05	0.15	0.77	2.31	8.23	5.58	1.30	0.17	0.13	0.20	99.69
Lujavrsite	53.41	1.22	15.28	6.66	2.30	0.46	1.35	1.79	9.48	4.65	1.18	0.31	0.14	0.03	98.26
Granite	71.30	0.31	14.32	1.21	1.64	0.05	0.71	1.84	3.68	4.07	0.64	0.13	0.12	0.05	100.07
Rhyolite	72.82	0.28	13.27	1.48	1.11	0.06	0.39	1.14	3.55	4.30	1.10	0.31	0.07	0.08	99.96
Quartz-monzonite	68.65	0.54	14.55	1.23	2.70	0.08	1.14	2.68	3.47	4.00	0.59	0.14	0.19	0.09	100.05
Granodiorite	66.09	0.54	15.73	1.38	2.73	0.08	1.74	3.83	3.75	2.73	0.85	0.19	0.18	0.08	99.90
Tonalite	61.52	0.73	16.48	1.83	3.82	0.08	2.80	5.42	3.63	2.07	1.04	0.20	0.25	0.14	100.01
Diorite	57.48	0.95	16.67	2.50	4.92	0.12	3.71	6.58	3.54	1.76	1.15	0.21	0.29	0.10	99.98
Andesite	57.94	0.87	17.02	3.27	4.04	0.14	3.33	6.79	3.48	1.62	0.83	0.34	0.21	0.05	99.93
Syenite	62.60	0.78	15.65	1.92	3.08	0.10	2.02	4.17	3.73	4.06	0.90	0.19	0.25	0.08	99.53
Trachy-andesite	58.15	1.08	16.70	3.26	3.21	0.16	2.57	4.96	4.35	3.21	1.25	0.58	0.41	0.08	99.97
Gabbro	50.14	1.12	15.48	3.01	7.62	0.12	7.59	9.58	2.39	0.93	0.75	0.11	0.24	0.07	99.15
Basalt	49.20	1.84	15.74	3.79	7.13	0.20	6.73	9.47	2.91	1.10	0.95	0.43	0.35	0.11	99.95
Tholeiitic basalt	49.58	1.98	14.79	3.38	8.03	0.18	7.30	10.36	2.37	0.43	0.91	0.50	0.24	0.03	100.08
Nephelinite	40.60	2.66	14.33	5.48	6.17	0.26	6.39	11.89	4.79	3.46	1.65	0.54	1.07	0.60	99.89
Tephrite	47.80	1.76	17.00	4.12	5.22	0.15	4.70	9.18	3.69	4.49	1.03	0.22	0.63	0.02	100.01
Anorthosite	50.28	0.64	25.86	0.96	2.07	0.05	2.12	12.48	3.15	0.65	1.17	0.14	0.09	0.14	99.80
Pyroxenolite	46.27	1.47	7.16	4.27	7.18	0.16	16.04	14.08	0.92	0.64	0.99	0.14	0.38	0.13	99.83
Peridotite	42.26	0.63	4.23	3.61	6.58	0.41	31.24	5.05	0.49	0.34	3.91	0.31	0.10	0.30	99.46
Dunite	38.29	0.09	1.82	3.59	9.38	0.71	37.94	1.01	0.20	0.08	4.19	0.25	0.20	0.43	98.18

mineral, as the previous calculations for the silicate and oxide minerals by Zheng (1991, 1993a,b).

(1) Calculation from the CIPW normative minerals: The relative abundances of normative minerals for the common magmatic rocks are calculated by using the conventional CIPW method based on their chemical compositions, and the results are listed in Table 2. The I-^{18}O index of a rock in question is defined by

$$\text{I-}^{18}\text{O}_{\text{rock}} = \sum X_{\text{mineral}} \times \text{I-}^{18}\text{O}_{\text{mineral}} \quad (1)$$

Where X_{mineral} denotes the mole fraction of oxygen atom in the normative mineral relative to the all minerals composed of this rock; I-^{18}O$_{\text{mineral}}$ is the oxygen isotope index of the mineral. It is noted that the I-^{18}O indices of diopside, hypersthene and olivine are also related to their Mg/Fe ratios. In order to simplify the calculation, the Mg/Fe ratio of whole rock is used to replace that of the minerals.

(2) Calculation from the normalized chemical composition: The chemical composition of the common magmatic rocks in Table 1 is normalized as oxides after eliminating H_2O^+, H_2O^-, P_2O_5 and CO_2, and the results are listed in Table 3. The I-^{18}O index of a rock is defined by

$$\text{I-}^{18}\text{O}_{\text{rock}} = \sum X_{\text{oxide}} \times \text{I-}^{18}\text{O}_{\text{oxide}} \quad (2)$$

where X_{oxide} denotes the mole fraction of oxygen atom in the oxide relative to all oxides composed of the rock after normalization; I-^{18}O$_{\text{oxide}}$ is the oxygen isotope index of the oxide. According to the increment method, the I-^{18}O index of oxide is essentially determined by the cation–oxygen bond strength and the cation mass (Schütze, 1980; Zheng, 1991). The I-^{18}O indices of the oxides used in this study are outlined in Table 4. It is known that Fe^{2+}, Mn^{2+} and Mg^{2+} are mostly distributed in the M1 and M2 sites of pyroxene and olivine for mafic and ultramafic rocks, and the frequency of M1 and M2 sites filled by these cations is almost the same. The cations in the M1 and M2 sites can differentially contribute ^{18}O-increments to I-^{18}O indices for pyroxenes and olivines, k=0 is thus assumed for the cations in M2 sites whereas k=−1 is assumed for the complex cations in M1 sites (Zheng, 1993a). By taking this difference into account, the I-^{18}O indices for FeO, MnO and MgO listed in Table 4 are the average in the case of k=−1 and k=0.

2.2. Thermodynamic oxygen isotope factors ($10^3 ln\beta$)

In the second step, the temperature-dependent thermodynamic isotope factors are calculated, which are expressed as β-factors and essentially correspond-

Table 2
The CIPW normative minerals of common magmatic rocks (%)

Rock	Q	C	Or	Ab	An	Lc	Ne	Ac	Ns	Di	Hy	Ol	Mt	Il	Ap	Cc	Total
Nepheline syenite	0	0	33.67	29.79	3.84	0	22.35	0	0	4.66	0	0.65	3.33	1.16	0.31	0.45	100.21
Lujavrsite	0	0	28.42	19.44	0	0	18.98	19.92	1.36	6.66	0	2.46	0	2.40	0.34	0.07	100.04
Granite	29.31	0.94	24.23	31.36	8.09	0	0	0	0	0	3.38	0	1.77	0.59	0.29	0.11	100.06
Rhyolite	33.41	1.08	25.84	30.48	4.75	0	0	0	0	0	1.44	0	2.19	0.54	0.17	0.18	100.08
Quartz-monzonite	25.27	0.31	23.81	29.57	11.57	0	0	0	0	0	6.08	0	1.80	1.03	0.45	0.20	100.10
Granodiorite	22.58	0.27	16.35	32.11	17.54	0	0	0	0	0	7.58	0	2.02	1.04	0.43	0.18	100.09
Tonalite	16.36	0	12.38	31.17	22.87	0	0	0	0	1.51	10.86	0	2.68	1.40	0.60	0.32	100.15
Diorite	10.43	0	10.53	30.42	24.78	0	0	0	0	4.75	12.77	0	3.68	1.83	0.70	0.23	100.12
Andesite	12.56	0	9.72	29.79	26.39	0	0	0	0	4.88	9.64	0	4.80	1.67	0.50	0.11	100.06
Syenite	14.23	0	24.42	32.05	14.21	0	0	0	0	3.81	6.26	0	2.83	1.52	0.60	0.18	100.09
Trachy-andesite	7.88	0	19.35	37.56	16.87	0	0	0	0	3.99	6.38	0	4.82	2.10	0.98	0.18	100.10
Gabbro	0.86	0	5.60	20.56	29.30	0	0	0	0	13.83	22.58	0	4.44	2.16	0.57	0.16	100.08
Basalt	0	0	6.63	24.97	27.07	0	0	0	0	14.24	15.55	1.43	5.58	3.55	0.84	0.25	100.13
Tholeiitic basalt	2.34	0	2.57	20.33	28.85	0	0	0	0	17.38	19.15	0	4.96	3.82	0.57	0.07	100.04
Nephelinite	0	0	3.01	0	7.61	14.14	22.60	0	0	33.38	0	2.54	8.19	5.21	2.62	1.36	100.66
Tephrite	0	0	26.88	8.76	16.78	0	12.39	0	0	20.05	0	4.22	6.05	3.38	1.51	0.05	100.05
Anorthosite	0.56	0	3.89	27.09	55.44	0	0	0	0	4.84	5.14	0	1.41	1.23	0.22	0.32	100.14
Pyroxenolite	0	0	3.83	7.87	13.73	0	0	0	0	42.65	6.34	15.43	6.28	2.82	0.91	0.30	100.15
Peridotite	0	0	2.10	4.33	8.82	0	0	0	0	11.79	16.70	48.86	5.51	1.27	0.25	0.68	100.31
Dunite	0	1.07	0.50	1.78	1.21	0	0	0	0	0	16.95	71.68	5.58	0.18	0.50	1.00	100.45

Q—quartz, C—corundum, Or—orthoclase, Ab—albite, An—anorthite, Lc—leucite, Ne—nepheline, Ac—acmite, Ns—Na-metasilicate, Di—diopside, Hy—hypersthene, Ol—olivine, Mt—magnetite, Il—illite, Ap—apatite, Cc—calcite.

ing to the reduced partition function ratios in the statistico-mechanical methods (Zheng, 1991). There are two cases that should be considered, respectively.

(1) With respect to the rapid cooling of extrusive melt or rapid crystallization of magma, the temperatures of magma solidification are significantly

Table 3
The normalized chemical compositions of the common magmatic rocks (%)

Rock	SiO_2	TiO_2	Al_2O_3	Fe_2O_3	FeO	MnO	MgO	CaO	Na_2O	K_2O
Nepheline syenite	56.18	0.61	21.41	2.30	2.09	0.15	0.79	2.36	8.41	5.70
Lujavrsite	55.29	1.26	15.82	6.89	2.38	0.48	1.40	1.85	9.81	4.81
Granite	71.93	0.31	14.45	1.22	1.65	0.05	0.72	1.86	3.71	4.11
Rhyolite	74.00	0.28	13.49	1.50	1.13	0.06	0.40	1.16	3.61	4.37
Quartz-monzonite	69.32	0.55	14.69	1.24	2.73	0.08	1.15	2.71	3.50	4.04
Granodiorite	67.03	0.55	15.95	1.40	2.77	0.08	1.76	3.88	3.80	2.77
Tonalite	62.53	0.74	16.75	1.86	3.88	0.08	2.85	5.51	3.69	2.10
Diorite	58.52	0.97	16.97	2.55	5.01	0.12	3.78	6.70	3.60	1.79
Andesite	58.82	0.88	17.28	3.32	4.10	0.14	3.38	6.89	3.53	1.64
Syenite	63.81	0.80	15.95	1.96	3.14	0.10	2.06	4.25	3.80	4.14
Trachy-andesite	59.55	1.11	17.10	3.34	3.29	0.16	2.63	5.08	4.45	3.29
Gabbro	51.17	1.14	15.80	3.07	7.78	0.12	7.75	9.78	2.44	0.95
Basalt	50.15	1.88	16.04	3.86	7.27	0.20	6.86	9.65	2.97	1.12
Tholeiitic basalt	50.39	2.01	15.03	3.43	8.16	0.18	7.42	10.53	2.41	0.44
Nephelinite	42.28	2.77	14.92	5.71	6.43	0.27	6.65	12.38	4.99	3.60
Tephrite	48.72	1.79	17.33	4.20	5.32	0.15	4.79	9.36	3.76	4.58
Anorthosite	51.17	0.65	26.32	0.98	2.11	0.05	2.16	12.70	3.21	0.66
Pyroxenolite	47.12	1.50	7.29	4.35	7.31	0.16	16.34	14.34	0.94	0.65
Peridotite	44.56	0.66	4.46	3.81	6.94	0.43	32.94	5.32	0.52	0.36
Dunite	41.12	0.10	1.95	3.86	10.07	0.76	40.75	1.08	0.21	0.09

Table 4
Oxygen isotopic indices of oxides (revised after Zheng, 1991)

Oxide	SiO_2	TiO_2	Al_2O_3	Fe_2O_3	FeO	MnO	MgO	CaO	Na_2O	K_2O
$I\text{-}^{18}O$	1.0000	0.6322	0.8697	0.4809	0.4140	0.4066	0.3555	0.2374	0.0701	0.0578

greater than 1000 K. In this case, the thermodynamic oxygen isotope factors ($10^3\ln\beta$) for the rock in question is linearly correlated to $1/T^2$ (Bottinga and Javoy, 1973; Zheng, 1997, 1999b) by the relation:

$$10^3\ln\beta = A \times 10^6/T^2 \quad (3)$$

where T is the absolute temperature (in K). The thermodynamic oxygen isotope factors for the rock can be directly calculated from its oxygen isotope index by the following relation:

$$10^3\ln\beta_{rock} = I\text{-}^{18}O_{rock} \times 10^3\ln\beta_{quartz} \quad (4)$$

in which

$$10^3\ln\beta_{quartz} = 11.83 \times 10^6/T^2 \quad (5)$$

where quartz is the reference mineral, $10^3\ln\beta_{quartz}$ values are based on the theoretical calculation of Kieffer (1982) at the temperatures above 1000 K as listed by Clayton et al. (1989) and given by Zheng (1997). In general, the closure temperature of oxygen isotope exchange between phenocryst and lava in volcanic rocks is usually higher than 1000 K, thus oxygen isotope fractionation factors ($10^3\ln\alpha$) between phenocryst and lava is expressed in the form of Eq. (3) by the relation:

$$10^3\ln\alpha_{phenocryst-lava} = 10^3\ln\beta_{phenocryst} - 10^3\ln\beta_{lava} \quad (6)$$

where $10^3\ln\beta_{phenocryst}$ is the thermodynamic oxygen isotope factor for the phenocryst mineral in question, which can be consulted in Zheng (1999b).

(2) With respect to subsolidus isotopic exchange between minerals and to possible water–rock interaction after magma crystallization, the temperatures involved can change continuously from those above

Table 5
Oxygen isotopic indices for common magmatic rocks and oxygen isotope fractionation between rocks and water calculated by the CIPW normative minerals

Rock	$I\text{-}^{18}O$	$10^3\ln\beta_{rock}$ (>1000 K)	$10^3\ln\beta_{rock}$ (0–1200 °C)			$10^3\ln\alpha_{rock-water}$ (0–1200 °C)		
		A	A	B	C	A	B	C
Nepheline syenite	0.8713	10.31	6.516	8.000	−3.66	4.322	−7.164	2.37
Lujavrsite	0.8606	10.18	6.496	7.804	−3.57	4.302	−7.359	2.42
Granite	0.9200	10.88	6.594	8.884	−4.08	4.400	−6.279	2.13
Rhyolite	0.9272	10.97	6.603	9.017	−4.14	4.409	−6.146	2.09
Quartz-monzonite	0.9122	10.79	6.583	8.740	−4.01	4.389	−6.423	2.17
Granodiorite	0.9029	10.68	6.569	8.570	−3.93	4.375	−6.593	2.21
Tonalite	0.8853	10.47	6.541	8.251	−3.78	4.347	−6.912	2.30
Diorite	0.8672	10.26	6.509	7.926	−3.63	4.315	−7.237	2.39
Andesite	0.8695	10.29	6.513	7.967	−3.65	4.319	−7.196	2.38
Syenite	0.8915	10.55	6.551	8.363	−3.83	4.357	−6.800	2.27
Trachy-andesite	0.8761	10.36	6.525	8.085	−3.70	4.331	−7.078	2.35
Gabbro	0.8234	9.74	6.417	7.160	−3.27	4.223	−8.003	2.59
Basalt	0.8227	9.73	6.416	7.148	−3.26	4.222	−8.015	2.60
Tholeiitic basalt	0.8184	9.68	6.406	7.074	−3.23	4.212	−8.089	2.62
Nephelinite	0.7887	9.33	6.331	6.572	−3.00	4.137	−8.591	2.75
Tephrite	0.8229	9.73	6.416	7.151	−3.27	4.222	−8.012	2.60
Anorthosite	0.8474	10.03	6.470	7.577	−3.47	4.276	−7.586	2.48
Pyroxenolite	0.7686	9.09	6.275	6.239	−2.84	4.081	−8.924	2.83
Peridotite	0.7311	8.65	6.158	5.635	−2.56	3.964	−9.528	2.98
Dunite	0.6975	8.25	6.041	5.113	−2.31	3.847	−10.050	3.11

Table 6
Oxygen isotopic indices for common magmatic rocks and oxygen isotope fractionations between rocks and water calculated by the normalized chemical composition

Rock	I-^{18}O	$10^3\ln\beta_{rock}$ (>1000 K)	$10^3\ln\beta_{rock}$ (0–1200 °C)			$10^3\ln\alpha_{rock-water}$ (0–1200 °C)		
		A	A	B	C	A	B	C
Nepheline syenite	0.8749	10.35	6.523	8.064	−3.69	4.329	−7.099	2.32
Lujavrsite	0.8543	10.11	6.484	7.698	−3.52	4.290	−7.465	2.42
Granite	0.9282	10.98	6.605	9.036	−4.15	4.411	−6.127	2.07
Rhyolite	0.9348	11.06	6.613	9.158	−4.20	4.419	−6.005	2.04
Quartz-monzonite	0.9183	10.86	6.592	8.853	−4.06	4.398	−6.311	2.12
Granodiorite	0.9099	10.76	6.579	8.687	−3.98	4.385	−6.476	2.16
Tonalite	0.8915	10.55	6.551	8.363	−3.83	4.357	−6.800	2.25
Diorite	0.8736	10.33	6.521	8.041	−3.68	4.327	−7.122	2.33
Andesite	0.8760	10.36	6.525	8.084	−3.70	4.331	−7.079	2.32
Syenite	0.8964	10.60	6.559	8.452	−3.87	4.365	−6.711	2.22
Trachy-andesite	0.8797	10.41	6.531	8.150	−3.73	4.337	−7.013	2.30
Gabbro	0.8315	9.84	6.436	7.300	−3.34	4.242	−7.863	2.53
Basalt	0.8287	9.80	6.429	7.251	−3.31	4.235	−7.912	2.54
Tholeiitic basalt	0.8264	9.78	6.424	7.212	−3.29	4.230	−7.951	2.55
Nephelinite	0.7792	9.22	6.305	6.414	−2.92	4.111	−8.749	2.75
Tephrite	0.8259	9.77	6.423	7.203	−3.29	4.229	−7.960	2.55
Anorthosite	0.8625	10.20	6.500	7.843	−3.59	4.306	−7.320	2.39
Pyroxenolite	0.7687	9.09	6.275	6.241	−2.84	4.081	−8.922	2.80
Peridotite	0.7322	8.66	6.162	5.652	−2.56	3.968	−9.511	2.95
Dunite	0.7004	8.29	6.051	5.157	−2.33	3.857	−10.006	3.07

1000 K to those below 1000 K. In this case, the temperature range of 0–1200 °C can be applied, and the thermodynamic oxygen isotope factor for the rock in question is expressed by the following algebra equation:

$$10^3\ln\beta = A \times 10^6/T^2 + B \times 10^3/T + C \quad (7)$$

Unlike Eq. (4), the term D is added to calculation of $10^3\ln\beta$ for the rock by the relation (Zheng, 1991):

$$10^3\ln\beta_{rock} = D \times \text{I-}^{18}\text{O}_{rock} \times 10^3\ln\beta_{quartz} \quad (8)$$

in which

$$10^3\ln\beta_{quartz} = 6.673 \times 10^6/T^2 + 10.398 \times 10^3/T - 4.78 \quad (9)$$

$$D = \exp[\Delta E \times (1 - \text{I-}^{18}\text{O}_{rock})/RT] \quad (10)$$

where R is the gas constant (8.31441 J K^{-1} mol^{-1}), $10^3\ln\beta_{quartz}$ values are based on the data of Kieffer (1982) as regressed by Zheng (1993a) at 0–1200 °C; ΔE is assumed to be an energy term in the Arrhenius expression, which has the value of 1 kJ mol^{-1} (Zheng, 1991). $10^3\ln\beta_{rock}$ can then be obtained through the regression in the functional form of Eq. (7). Unlike the above calculations of the fractionation factors for the phenocryst–lava systems by Eq. (6), a term of the β-factor for rock–water interaction ($10^3\ln\beta_{r-w}$) is added when calculating the $10^3\ln\alpha$ values for rock–water systems (Zheng, 1993a). Oxygen isotope fractionation factors between rock and water are then expressed as:

$$10^3\ln\alpha_{rock-water} = 10^3\ln\beta_{rock} - 10^3\ln\beta_{water} + 10^3\ln\beta_{r/w} \quad (11)$$

in which

$$10^3\ln\beta_{water} = 2.194 \times 10^6/T^2 + 15.163 \times 10^3/T - 4.72 \quad (12)$$

$$10^3\ln\beta_{r/w} = 1.767(2 \times \text{I-}^{18}\text{O}_{rock} - 1) \quad (13)$$

Table 7
Oxygen isotope fractionation in phenocryst–lava systems calculated by the CIPW normative minerals ($10^3\ln\alpha_{\text{phenocryst-lava}}=A\times10^6/T^2$)

Rock	Q	Or	Ab	An	Ne	Ac	Di	Hy	Ol	Mt	Il	Ap
Rhyolite	0.86	−0.23	−0.15	−1.18	–	–	–	–	–	−4.58	−4.90	−0.91
Andesite	–	0.45	0.53	−0.49	–	−0.22	−1.23	−1.03	–	−3.89	−4.22	−0.23
Trachy-andesite	–	0.37	0.46	−0.57	–	−0.30	−1.30	−1.11	–	−3.97	−4.29	−0.31
Basalt	–	1.00	1.09	0.06	–	0.34	−0.67	−0.48	−1.70	−3.34	−3.66	0.32
Tholeiitic basalt	–	1.05	1.14	0.11	–	0.39	−0.62	−0.43	−1.65	−3.29	−3.61	0.37
Nephelinite	–	1.41	–	–	0.44	0.74	−0.27	−0.08	–	−2.94	−3.26	0.73
Tephrite	–	1.00	1.09	0.06	0.03	–	−0.67	–	−1.70	−3.34	−3.66	0.32

where $10^3\ln\beta_{\text{water}}$ values were regressed from the data listed by Hattori and Halas (1982) as regressed by Zheng (1993a). The rock–water interaction term is used to correspond to the mineral–water interaction term in order to cancel out the isotopic effects of dissolved minerals in aqueous solutions and dissolved water as hydroxyl in minerals. This reconciles the discrepancy between theoretically calculated and experimentally measured fractionation factors for the silicate–water system to bring them into the best available agreement (Zheng, 1993a).

(3) With respect to CO_2 degassing during magma emplacement, the temperatures involved can change largely from those above 1000 K to those below 1000 K. Thermodynamic oxygen isotope factor for melts is assumed to be represented by that for rocks of the same composition and thus expressed by Eqs. (7) and (8). Because CO_2 can be dissolved either as molecular form in silicic melts or as $[CO_3]^{2-}$ in mafic melts, a term of the β-factor for CO_2–melt interaction ($10^3\ln\beta_{c-m}$) is introduced to cancel out the isotopic effects of dissolved CO_2 or $[CO_3]^{2-}$ in melts when calculating the $10^3\ln\alpha$ values for CO_2–melt systems. Like the above calculations of the fractionation factors for the rock–H_2O systems by Eq. (11), oxygen isotope fractionation between CO_2 and melt is then expressed as:

$$10^3\ln\alpha_{CO_2-\text{melt}} = 10^3\ln\beta_{CO_2} - 10^3\ln\beta_{\text{melt}} + 10^3\ln\beta_{c/m} \quad (14)$$

in which

$$10^3\ln\beta_{CO_2} = 5.112\times10^6/T^2 + 18.154\times10^3/T - 6.79 \quad (15)$$

$$10^3\ln\beta_{c/m} = -0.883(2\times I\text{-}^{18}O_{\text{melt}} - 1) \quad (16)$$

where $10^3\ln\beta_{CO_2}$ values were regressed from the data listed by Chacko et al. (1991) in a temperature range of 0–1500 °C, and 0.883 is obtained by dividing the factor 1.767 by 2 in $10^3\ln\beta_{r-w}$ because of two oxygen atoms in CO_2 relative to one oxygen atom in H_2O.

3. Results

Oxygen isotope fractionation factors ($10^3\ln\alpha$) between magmatic rocks and water and between

Table 8
Oxygen isotope fractionation in phenocryst–lava systems calculated by the normalized chemical composition ($10^3\ln\alpha_{\text{phenocryst-lava}}=A\times10^6/T^2$)

Rock	Q	Or	Ab	An	Ne	Ac	Di	Hy	Ol	Mt	Il	Ap
Rhyolite	0.77	−0.32	−0.24	−1.26	–	–	–	–	–	−4.67	−4.99	−1.00
Andesite	–	0.37	0.46	−0.57	–	−0.29	−1.30	−1.11	–	−3.97	−4.29	−0.31
Trachy-andesite	–	0.33	0.41	−0.61	–	−0.34	−1.34	−1.15	–	−4.01	−4.34	−0.35
Basalt	–	0.93	1.02	−0.01	–	0.27	−0.74	−0.55	−1.77	−3.41	−3.73	0.25
Tholeiitic basalt	–	0.96	1.04	0.02	–	0.29	−0.72	−0.52	−1.74	−3.38	−3.71	0.28
Nephelinite	–	1.52	–	–	0.55	0.85	−0.16	0.03	–	−2.83	−3.15	0.84
Tephrite	–	0.96	1.05	0.02	−0.01	–	−0.71	–	−1.74	−3.38	−3.70	0.28

phenocrysts and lava are calculated on the basis of the calculated CIPW normative minerals and normalized chemical composition, oxygen isotope indices (I-^{18}O), and the temperature-dependent thermodynamic isotope factors ($10^3 \ln\beta$). The results are listed in Tables 5–8. Figures 1 and 2 depict the relationship of

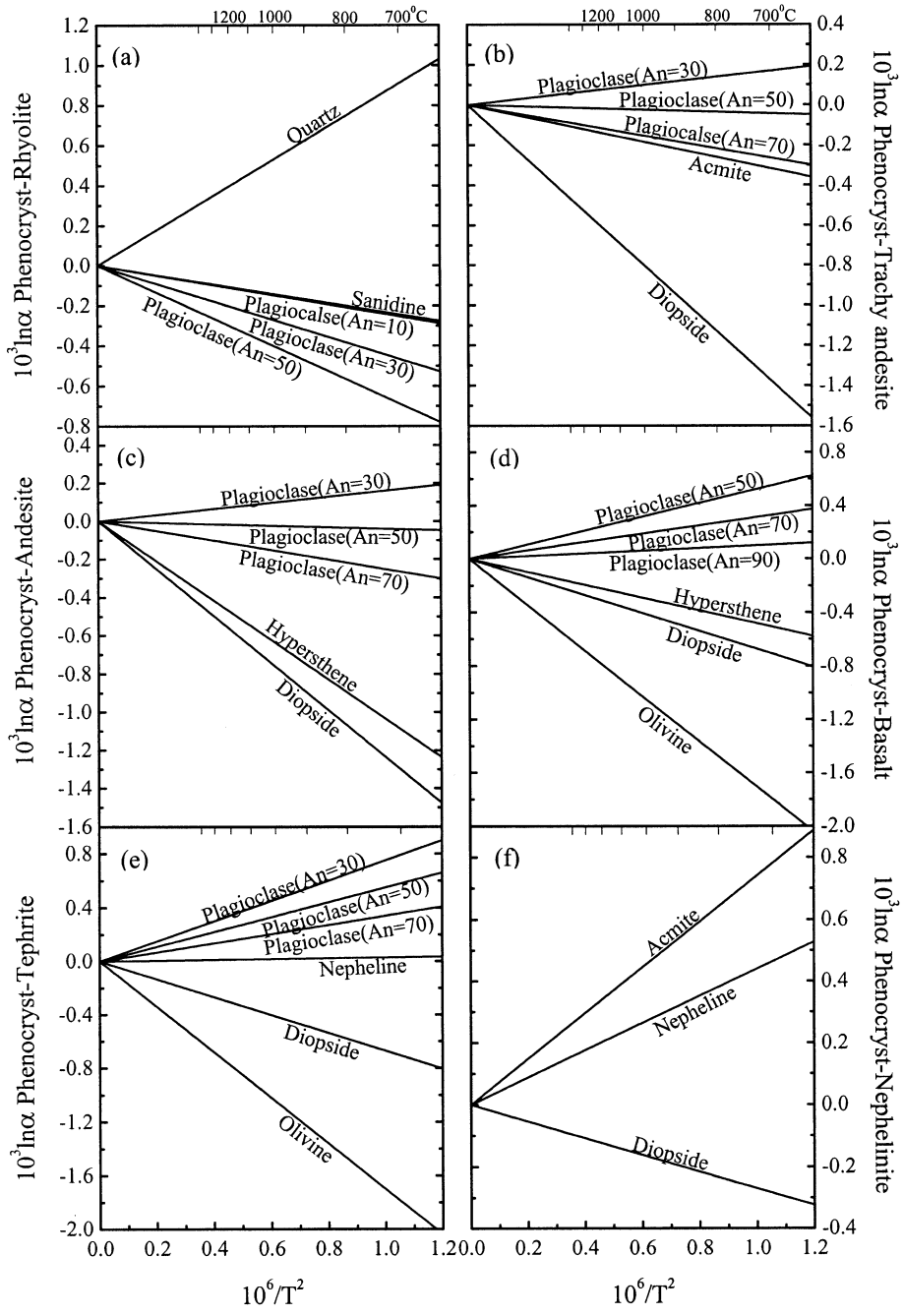

Fig. 1. Theoretically calculated oxygen isotope fractionation factors between phenocryst and lava.

temperature to oxygen isotope fractionations between phenocryst and lava and between the common magmatic rocks and water, respectively. The error contributed to the fractionation relations involving the magmatic rocks is estimated to be within ±2% following the modified increment method, as previously given by Zheng (1991) for the metal oxides and Zheng (1993a) for the silicate minerals.

In terms of the size of I-^{18}O indices, the order of ^{18}O enrichment in the magmatic rocks can be predicted as follows: rhyolite ≈ granite > quartz monzonite > diorite > syenite > tonalite > andesite ≈ diorite > anorthosite > gabbro ≈ basalt > tholeiitic basalt > pyroxenolite > peridotite > dunite. The volcanic rocks have almost the same I-^{18}O indices as their chemical counterparts in crystalline phase.

The present results for the phenocryst–lava systems (Fig. 1) indicate that the curves of both thermodynamic isotope factors for the magmatic rocks and isotopic fractionation factors are radically divergent from the origin to varying slopes and are zero at infinite temperature. This implies that neither crossover nor intersection can occur between the fractionation curves of the different phenocrysts–lava systems. For the rock–water systems (Fig. 2), however, most of the fractionation curves pass through a minimum (i.e., the negative value for $10^3\ln\alpha$) before approaching the origin, similar to the results for the metal oxides and anhydrous silicates (Zheng, 1991, 1993a). For the hydrothermal alteration of magmatic rocks by surface fluids (seawater or meteoric water), a general ^{18}O depletion in altered rocks is thus expected at high-T equilibrium conditions because the oxygen isotope fractionations between rocks and water are generally less than or equal to zero at the temperatures above 400 to 600 °C depending on rock composition.

4. Discussions

4.1. Relationship in I-^{18}O of magmatic rocks between the two calculation methods

The oxygen isotope indices (I-^{18}O) of the common magmatic rocks are calculated by the two approaches in this study, i.e., calculations on the CIPW normative minerals and the normalized chemical composition. They are basically responsible for the crystalline intrusive rocks and noncrystalline extrusive rocks. Theoretically, the results are not

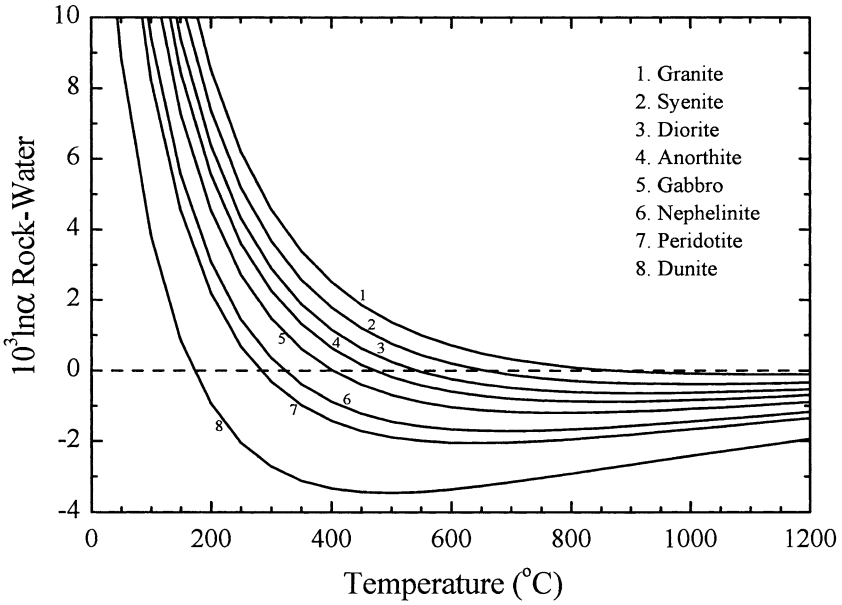

Fig. 2. Theoretically calculated oxygen isotope fractionation factors between the common magmatic rocks and water.

independent of the calculation methods because of the same starting chemical compositions, and thus should be identical with each other within the calculation errors. As depicted in Fig. 3, the results obtained from the two approaches are indeed in excellent agreement with each other, demonstrating that both the CIPW normative minerals and the normalized chemical composition can yield the reasonable fractionation factors of oxygen isotopes in the magmatic rocks. In fact, the some features of crystal structure (e.g., Fe^{2+}, Mg^{2+} and Mn^{2+} in M1 and M2 sites for pyroxene and olivine) have been considered in the calculation of the normalized chemical composition. The consistent results from the two approaches suggest negligible oxygen isotope fractionation between rock and melt of the same compositions. The similar consistency was also observed for the CO_2–glass fractionations concerning melt and mineral of albitic and anorthitic composition (Matthews et al., 1998). Therefore, the oxygen isotopic properties of melts can be represented by the incremental values for different types of bonds in the crystalline state.

Some approximations have been introduced to simplify the calculations. For the calculation from the CIPW normative minerals, the simplifications are: (1) hydroxyl-bearing minerals were not included; (2) the ratio of Mg/Fe in whole rock was used to represent that in pyroxene and olivine; and (3) 0.85 and 0.95 were empirically used as I-^{18}O values of apatite and calcite, respectively, which belong to the other series with calcite as a reference mineral (Zheng, 1996, 1999a). These approximations can only introduce very small differences in the resultant oxygen isotope fractionation factors because the amounts of hydroxyl-bearing minerals, apatite and calcite are small in the common fresh magmatic rocks, and because there are very small differences in I-^{18}O between enstatite and ferrosilite and between forsterite and fayalite (Zheng, 1993a).

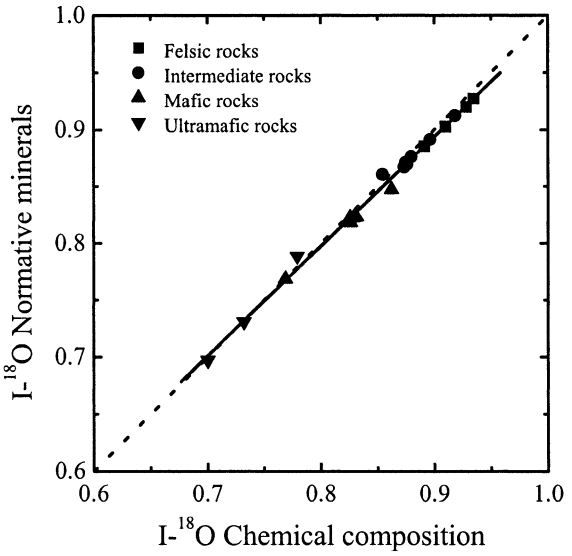

Fig. 3. Comparison of oxygen isotope indices calculated from the CIPW normative minerals with those from the normalized chemical composition for the common magmatic rocks.

For the calculation from the normalized chemical composition, the approximations are: (1) fixed coordination number of cations was used for given oxides, although the cations may have different coordination numbers in various minerals (e.g., the coordination number of K^+ in K-feldspar is 10, but 6 in leucite and 9 in nepheline); (2) volatile component including CO_2, H_2O and P_2O_5 were excluded when normalizing the chemical composition of the magmatic rocks. These simplifications have not brought large errors to the calculated results because many of the cations have single coordination number in the common minerals (e.g., the coordination numbers of Fe^{2+} and Mg^{2+} in pyroxene and olive are 6) and because the contents of the volatile components are always very small in the common fresh magmatic rocks. The agreement in Fig. 3 suggests that the presence or absence of the volatile components does not significantly influence the intrinsic property of oxygen isotope fractionation in the magmatic rocks.

Because the results obtained from the two approaches (the CIPW normative minerals and the normalized chemical composition) are almost the same within the analytical uncertainty, only the results from the CIPW normative minerals are illustrated in the following discussion. In dealing with naturally occurred rocks, nevertheless, either of them can be applied without preference for the purpose of processing them in a convenient and quick way to acquire the oxygen isotope indices of and thus the fractionation factors for the natural rocks in question.

4.2. Relationship between I-^{18}O and SiO_2 content

Empirically, the degree of the ^{18}O enrichment in magmatic rocks increases with increasing SiO_2 content because SiO_2 is enriched in ^{18}O. As shown in Fig. 4, this consensus is in fair agreement with the theoretical consideration. However, a simple linear relationship between I-^{18}O and SiO_2 is not observed because the chemical compositions besides SiO_2 are significantly different in the magmatic rocks and thus are variably contributed to the I-^{18}O indices. A polynomial regression is performed for the data in Fig. 4, and the relationship between I-^{18}O and SiO_2 content is thus expressed as follows:

$$y = 0.0497 + 0.0230x - 1.518 \times 10^{-4}x^2 \qquad (17)$$

where y represents the I-^{18}O index of the magmatic rocks, and x denotes the SiO_2 content. Eq. (17) can be used to roughly estimate the I-^{18}O index of a magmatic rock whose SiO_2 content falls within the range of 35–80%, but uncertainty is large either in the I-^{18}O range insensitive to SiO_2 variation or in the SiO_2 range insensitive to I-^{18}O variation.

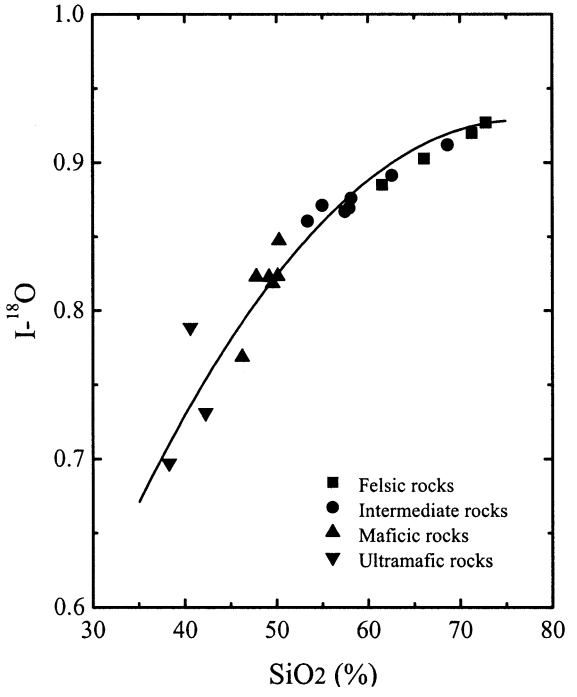

Fig. 4. Relationship between oxygen isotope indices and SiO_2 contents of the common magmatic rocks.

As depicted in Fig. 1 and oxygen isotope fractionation equations listed in Tables 7 and 8, ferromagnesian minerals (e.g., pyroxene and olivine) are often depleted in ^{18}O relative to their hosted lava, but felsic minerals (e.g., quartz and feldspar) are usually enriched in ^{18}O compared to their hosted lava (except the feldspar–rhyolite system). The major difference between ferromagnesian and felsic minerals is that the latter contain more SiO_2 than the former, corresponding to the following sequence of ^{18}O-enrichment: felsic rocks > intermediate rocks > mafic rocks > ultramafic rocks. This is not only theoretically correct, but also consistent with the natural observations (Taylor and Epstein, 1962; Garlick, 1966; Taylor, 1968; Anderson et al., 1971).

As shown in Fig. 2, oxygen isotope fractionations between magmatic rocks and water become lower and lower when the rock composition changes from granite to dunite. As a result, the magnitude of oxygen isotope fractionations vary at the same temperature: rhyolite–water > andesite–water > basalt–water > peridotite–water.

5. Comparison with known data

In order to test the accuracy of the present calculations, comparison between the calculated fractionations and known experimental and/or empirical calibrations can be made in one of the three ways: (1) rock–water systems, (2) phenocryst–lava systems, and (3) CO_2–melt/glass systems.

5.1. Rock–water system

Cole et al. (1987) experimentally determined oxygen isotope fractionations between altered basalt and water in the temperature range of 300–500 °C by use of the partial exchange technique. As depicted in Fig. 5, the results of Cole et al. (1987) are significantly greater than the present calculations for the basalt–water system, but in good agreement with those for the plagioclase (An=30)–water system.

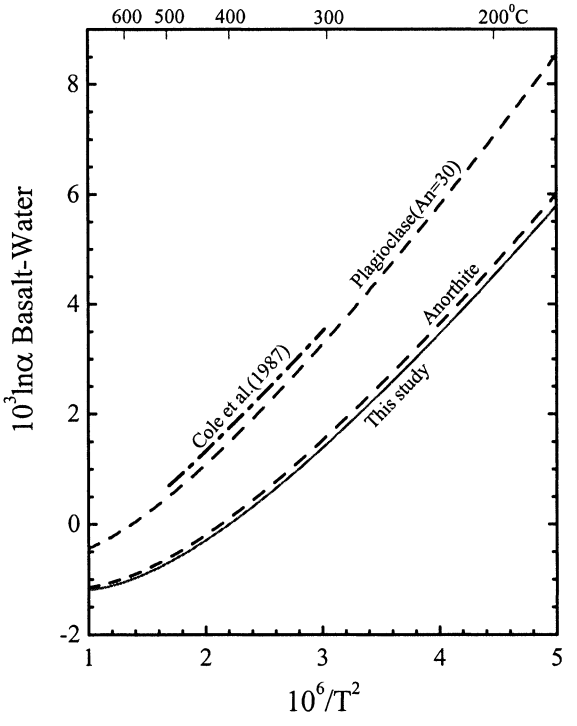

Fig. 5. Comparison of oxygen isotope fractionation factors between basalt and water calculated in this study with those from the experimental determination of Cole et al. (1987). The data for the feldspar–water systems are after Zheng (1993a).

However, the present calculations for the basalt–water system compare well with those for the anorthite–water system. It is known that there are significant differences in chemical composition and mineral assemblage between fresh and altered basalts because of chemical transfer and mineralogical transformation during basalt–seawater interaction. The laboratory experiments predicted that the major chemical exchange that occurs during basalt–seawater interaction is substitution of seawater Mg for basalt Ca (Mottl, 1983). Because MgO has an I-^{18}O index larger than CaO (Table 4), this is the reason why the experimental fractionations by Cole et al. (1987) for the altered basalt–water system are greater than the present calculations for the fresh basalt–water system (Fig. 5). Additionally, the isotopic effect of dissolved salt was not corrected by Cole et al. (1987), which can also have influenced their results. Pressure effect may be negligible for crustal rocks at low pressures (Clayton, 1981; O'Neil, 1986).

According to the proportions of alteration minerals for the systems in which basalt reacts with seawater at different water/rock ratios as computed by Mottl (1983) and Reed (1983), Cole et al. (1987) estimated oxygen isotope fractionations between altered basalt and water by combining the appropriate mineral–water equilibrium fractionation factors for each alteration phase with their proportions. Although there are some differences between the alteration mineralogy observed in the experiments and the phase assemblages given by Mottl (1983) and Reed (1983), there is a fair agreement between the experimental calibrations and calculated results (Cole et al., 1987). Bowers and Taylor (1985) estimated oxygen isotope fractionations between altered basalt and water from computer modeling for mass transfer reactions, which compare well with the present calculations for the basalt–water system (not shown in Fig. 5 of this study, but clear when comparing Fig. 6 of Cole et al., 1987 with Fig. 14 of Bowers and Taylor, 1985).

Cole et al. (1992) experimentally investigated variations in alteration mineralogy and the oxygen isotopic composition of solutions, minerals, and rocks with time in the system granite–$H_2O\pm$ NaCl$\pm$KCl at 170–300 °C. Alteration mineral assemblages formed in the experiments were chlorite (after biotite), sericite–zeolite–albite (after K-feldspar and plagioclase), and hematite (after magnetite and pyrite). Because the final equilibrium mineral assemblages were not attained in the experiments, the computer programs on mass transfer developed by Wolery (1978, 1979, 1983) were used to calculate the equilibrium mineral assemblages between the granites and fluids. Oxygen isotope fractionation factors between granitic gneiss and water and between biotite quartz monzonite and water in the temperature range of 170–300 °C were thus calculated by combining the appropriate mineral–water equilibrium fractionation factors for each phase with their mineral proportions. As shown in Fig. 6, the present calculations are in a good agreement with the results of Cole et al. (1992). The present results for granite and quartz monzonite are compared with the granitic gneiss and the biotite quartz monzonite, respectively,

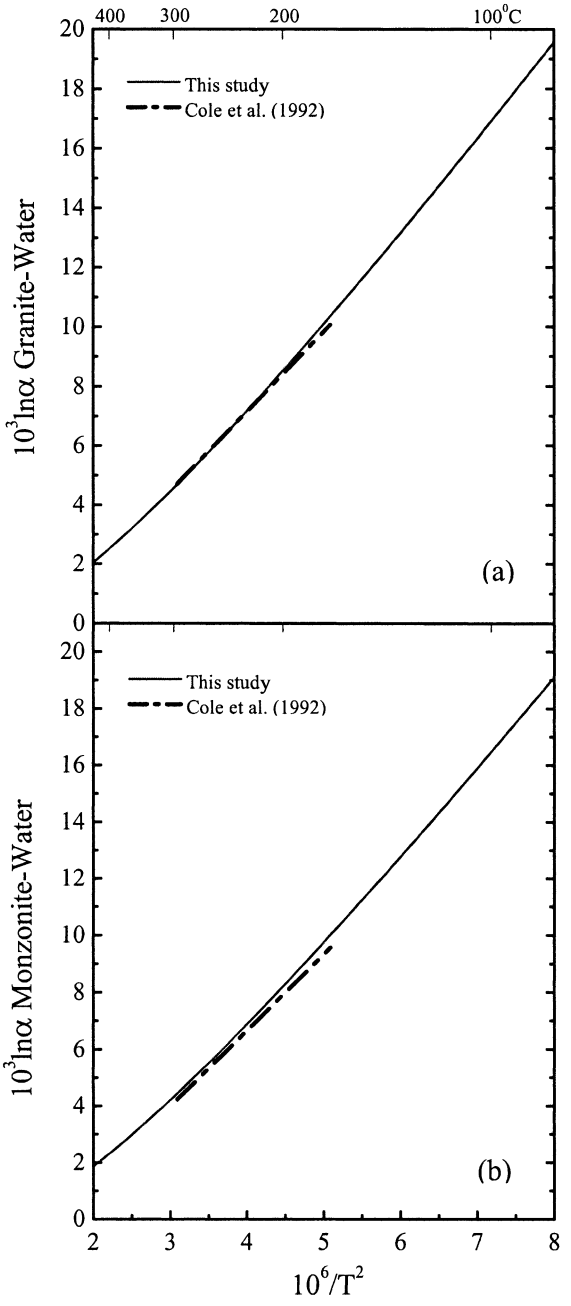

Fig. 6. Comparison of oxygen isotope fractionations between granite and water calculated in this study with the experimental calibrations of Cole et al. (1992).

because of close similarity in their chemical compositions (compare Appendix A of Cole et al., 1992 with Table 1 of this study).

5.2. Phenocryst–lava system

By employing the Kiglapait $\delta^{18}O$ whole-rock and liquid trends, published intra-mineral fractionation factors, and material balance, Kalamarides (1986) empirically estimated oxygen isotope fractionations between phenocrysts and basalt at 1443 K and between phenocrysts and dolerite at 1200–1550 K, respectively. As depicted in Fig. 7, oxygen isotope fractionations between plagioclase, pyroxene, olivine, Fe–Ti oxide (50% magnetite and 50% ilmenite) and basalt at 1443 K are 0.3‰, −0.2‰, −0.6‰ and −1.9‰, respectively, being in good agreement with the present calculations of 0.28‰, −0.23‰, −0.75‰ and −1.8‰. The results involving fayalite and magnetite (spinel structure) from this study are comparable to those by Kalamarides (1986) (Fig. 7c and d). Additionally, the present calculations also match the known observations from natural samples, as shown in Fig. 7 by the rectangle. Only exception is the feldspar–basalt system (Fig. 7a), whose fractionations are located at the low end of the published values, but still within the reported range.

As depicted in Fig. 8, the present calculations well match the fractionations between phenocrysts and dolerite empirically obtained by Kalamarides (1986). For the feldspar–dolerite system, however, the empirical calibration is consistently higher than this calculation at lower temperature, but still lies in the range for plagioclase with An=50–90% (Fig. 8a). The plagioclase with An=50–90% are used to plot because labradorite (An=50–70%) and bytownite (An=70–90%) are common in basalts. The calculation involving the magnetite of spinel structure (Zheng, 1995) is better comparable than that involving the magnetite of inverse-spinel structure with the empirical calibration (Fig. 8d). So is fayalite for olivine (Fig. 8c).

On the basis of a variety of oxygen isotope studies of volcanic rocks, Taylor and Sheppard (1986) concluded that: (1) the crystal–melt fractionations are small (<2‰) for the common rock-forming minerals such as quartz, feldspar, pyroxene, olivine, biotite, hornblende, leucite; (2) the plagioclase–melt $\Delta^{18}O$ values change from negative in rhyolites (0.1‰ to 0.5‰) to positive in basalts (−0.2‰ to −0.6‰) in spite of the fact that the

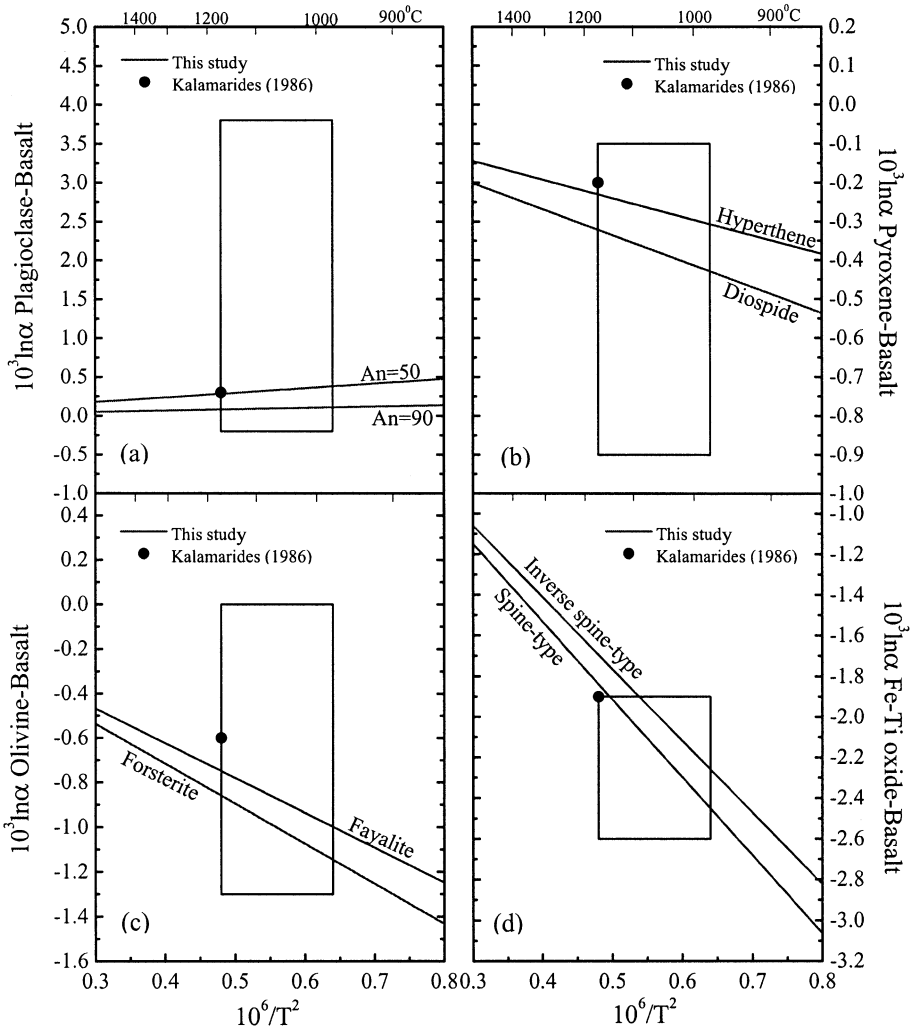

Fig. 7. Comparison of oxygen isotope fractionations between phenocryst and basaltic lava calculated in this study with the empirical data by Kalamarides (1986). Squares outline the empirical data from natural observations by Taylor (1968), O'Neil and Adami (1970), Anderson et al. (1971), Clayton et al. (1971), Epstein and Taylor (1971), Muehlenbachs and Clayton (1972), and Kyser et al. (1981, 1982).

reverse effect would a prior be predicted solely in terms of the chemical variation of the plagioclase. This feature clearly requires that the isotopic properties of the silicate melt change with its chemical composition, which can be easily understood from this study (Tables 5 and 6). As shown in Figs. 7 and 8, the present calculations are in a fair agreement with all of those results derived from the natural systems.

5.3. CO_2–melt system

Oxygen isotope fractionation involving magmatic melts was firstly measured by Muehlenbachs and Kushiro (1974) by exchanging CO_2 or O_2 with a basaltic melt at 1250–1550 °C and 1 atm. Additionally, plagioclase and enstatite were isotopically equilibrated with O_2 to obtain fractionation factors similar those achieved in CO_2. As a result, equilibrium

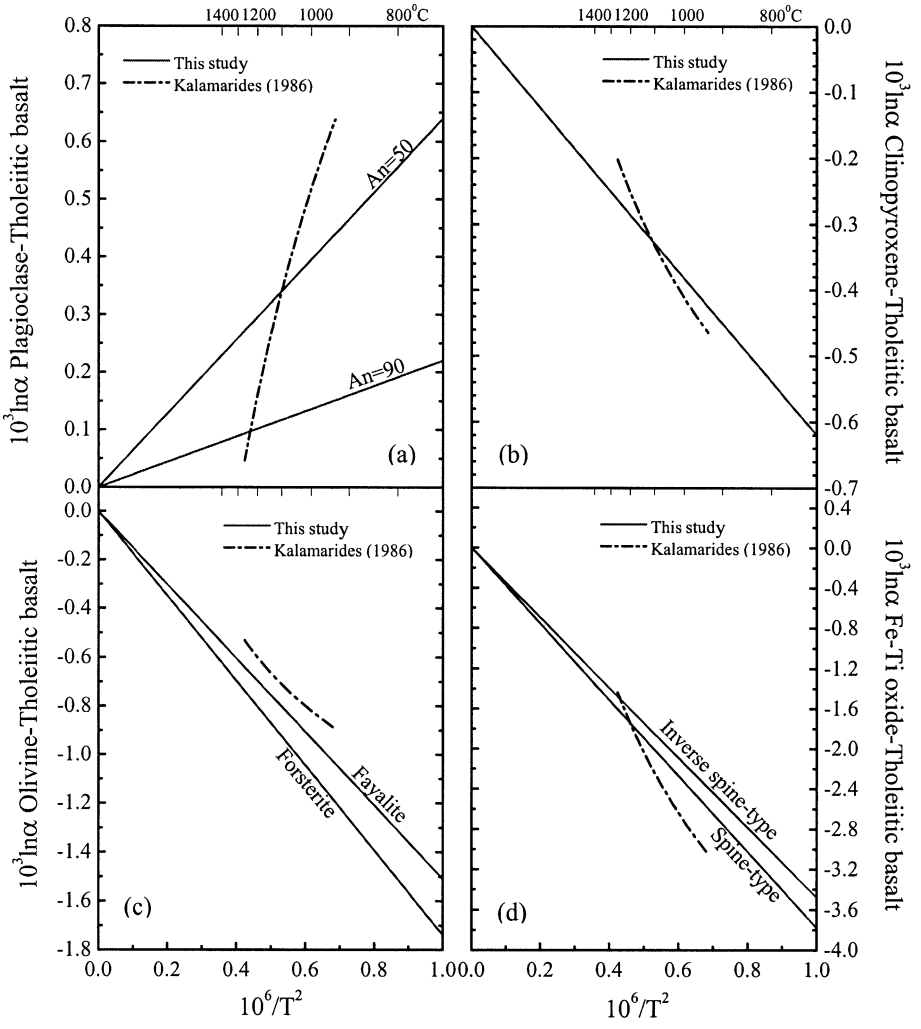

Fig. 8. Comparison of oxygen isotope fractionations between phenocryst and tholeiitic lava calculated in this study with the empirical data by Kalamarides (1986).

fractionations between plagioclase and the basaltic melt and between enstatite and the basaltic melt were estimated, respectively, to be −0.1‰ to 0.4‰ and −0.5‰ to 0.6‰ with large accumulated uncertainties. The presently calculated fractionations of 0.3‰ to 0.5‰ for the plagioclase–basalt system lie in the high end of the experimental values at the same temperature range, whereas the calculated fractionations of −0.2 to −0.3‰ for the enstatite–basalt system lie in the low end of the experimental values. The nature of correlations between the phenocryst–basalt fractionation and $10^6/T^2$ is consistent between the theoretical and experimental calibrations: the positive slope for the plagioclase–basalt system but the negative slope for the enstatite–basalt system.

Appora et al. (2000) measured oxygen isotope fractionations between CO_2 vapor and Na-melilite melt at 1250–1400 °C and 1 bar. The Na-rich melt was considered to correspond to a mineral end member with melilite stoichiometry and thus a good analog for natural olivine tholeiites. The authors obtained an oxygen isotope fractionation between plagioclase and soda-mililite melt of 0.1–0.5‰ at 1250 °C which is similar to the calculated fractionation between plagio-

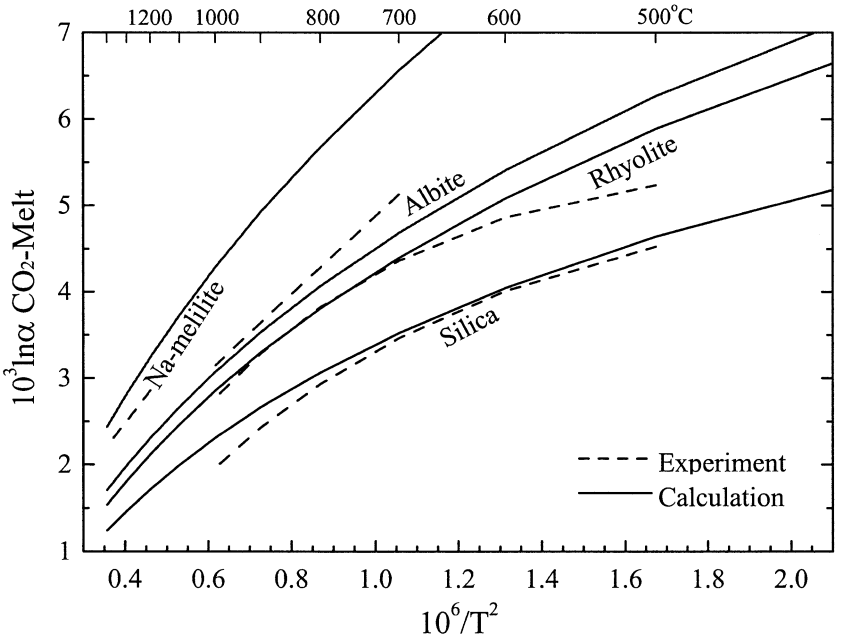

Fig. 9. Comparison of oxygen isotope fractionations between CO_2 and melt calculated by the increment method with the experimental data (data sources are after Table 9).

clase and tholeiitic basalt of 0.5‰ in this study. A combined fractionation between olivine and soda-mililite melt of −0.6‰ to −1.0‰ was estimated by Appora et al. (2000) at 1300 °C, which is in good agreement with the calculated fractionation between olivine and tholeiitic basalt of −0.7‰ from this study.

Oxygen isotope fractionations between gaseous CO_2 and a natural rhyolitic melt/glass were experimentally measured by Palin et al. (1996) at 550–950

Table 9
Regressed equations for oxygen isotope fractionation factors between CO_2 and melt

Melt	Fractionation equation	Temperature (°C)	Reference
Experiment			
Silica	$10^3\ln\alpha=-4.36\times10^6/T^2+14.11\times10^3/T-6.43$	550–950	1+2
Albite	$10^3\ln\alpha=4.52\times10^6/T^2+0.36$	750–950	2
Na-melilite	$10^3\ln\alpha=6.2\times10^6/T^2$	1250–1400	3
Rhyolite	$10^3\ln\alpha=-6.49\times10^6/T^2+18.35\times10^3/T-7.64$	550–950	4
Calculation			
Quartz	$10^3\ln\alpha=-1.56\times10^6/T^2+7.75\times10^3/T-2.89$	0–1500	5+6
Albite	$10^3\ln\alpha=-1.42\times10^6/T^2+9.14\times10^3/T-3.31$	0–1500	6+7
Anorthite	$10^3\ln\alpha=-1.20\times10^6/T^2+10.48\times10^3/T-3.73$	0–1500	6+7
Diopside	$10^3\ln\alpha=-1.00\times10^6/T^2+11.42\times10^3/T-4.01$	0–1500	6+7
Na-melilite	$10^3\ln\alpha=-1.04\times10^6/T^2+11.19\times10^3/T-3.94$	0–1500	6+7
Rhyolite	$10^3\ln\alpha=-1.49\times10^6/T^2+9.13\times10^3/T-3.39$	0–1500	6+8
Andesite	$10^3\ln\alpha=-1.40\times10^6/T^2+10.18\times10^3/T-3.79$	0–1500	6+8
Basalt	$10^3\ln\alpha=-1.31\times10^6/T^2+11.01\times10^3/T-4.10$	0–1500	6+8
Peridotite	$10^3\ln\alpha=-1.05\times10^6/T^2+12.52\times10^3/T-4.64$	0–1500	6+8

(1) Stolper and Epstein (1991). (2) Matthews et al. (1994). (3) Appora et al. (2000). (4) Palin et al. (1996). (5) Clayton et al. (1989). (6) Chacko et al. (1991). (7) Zheng (1993a). (8) This study.

°C and approximately 1 bar. Their results can be represented by fitting the experimental data in the form of a polynomial equation:

$$10^3\ln\alpha = -6.49 \times 10^6/T^2 + 18.35 \times 10^3/T - 7.64 \quad (18)$$

As depicted in Fig. 9, the experimental fractionations at the temperatures above about 600 °C are in general agreement with the calculated values for the CO_2–rhyolite system. Table 9 lists the regressed equations for the experimental data available for rhyolite, silica, albite and Na-melilite. Also listed in Table 9 are the calculated fractionations concerning quartz, albite, anorthite, diopside, Na-melilite (50% normative wollastonite+50‰ normative nepheline), rhyolite, andesite, basalt and peridotite in the polynomial form of $10^3\ln\alpha$ versus both $10^6/T^2$ and $10^3/T$. Figure 9 illustrates the general agreements between the experimental and calculated fractionations in the systems involving silica, albite and Na-melilite. It appears that the introduction of the CO_2–melt interaction term in Eq. (14) has reconciled the discrepancy between theoretically calculated and experimentally measured fractionation factors for the CO_2–melt systems to bring them into the best available agreement.

6. Applications to natural systems

Although our knowledge in oxygen isotope fractionation factors is reasonably good for various kinds of minerals (see summary by Zheng, 1999b), there have been basically little useful data for oxygen isotope fractionation in the crystal–melt and magma–water systems. By combining the present calculations with the mechanism and rate of isotopic exchange between rock and fluid under various geological conditions, the oxygen isotopic composition of magmatic rocks and involved crystals and fluids can be used as a quantitative tool in deciphering the geochemical history of natural magma differentiation and hydrothermal alteration. The present calculations show that oxygen isotope fractionations among silicate melts, their phenocrysts and exsolved gases, and minerals in their residues are similar in magnitude to those among mineral phases and fluids (H_2O or CO_2) small at magmatic temperatures. They are small for the phenocryst–phenocryst and phenocryst–lava systems (Fig. 1) and can be neglected in studies examining large variations in $\delta^{18}O$, such as those exhibited by some suites of crustally contaminated magmatic rocks. However, the fractionations involving the fluids can be quite large even at high temperatures (Figs. 2 and 9) and thus must be taken into account when interpreting oxygen isotope data for mantle-derived or altered rocks.

Application of calculated fractionation curves to natural systems has been a classical subject in reporting the new calculation results. Inasmuch as the present calculations are in a fair agreement with the known empirical and experimental calibrations, consistent results can generally be anticipated when applying the new calculations to natural magmatic rocks. Agreements between the theoretical calculations and the experimental determinations involving various minerals of metal oxide and hydroxide, anhydrous and hydroxyl-bearing silicates, wolframite and carbonate were clearly demonstrated in the previous publications (Zheng, 1991, 1993a,b, 1997, 1999a; Bird et al., 1993; Zhang et al., 1994; Rosenbaum and Mattey, 1995; Xu and Zheng, 1998; Zhou and Zheng, 2002). It is thus considered redundant to list some examples for illustrating the applicability of the present results to selected magmatic rocks.

Fractional crystallization is one of the important processes during magma cooling, by which several series of magmatic rocks were produced, for instance, the Hachijo-jima island arc volcanics (Matsuhisa, 1979), Galapagos Spreading Center (Muehlenbachs and Byerly, 1982), Ascension Island just off the Mid-Atlantic Ridge (Sheppard and Harris, 1985), rock 12013 of Apollo 12 (Taylor and Epstein, 1970), Easter Island (Taylor, 1968), and the Kiglapait intrusion, Labrador (Taylor, 1968; Kalamarides, 1984). During magma solidification, the controlling parameters for the oxygen isotope composition of minerals and melts are: (1) the oxygen isotope fractionation factors between crystals and melt, (2) the degree of isotopic reequilibration between crystals and melt, and (3) the modal variations or relative abundances of the various minerals crystallizing which are determined by the positions of multi-component cotectics in the pertinent phase equilibrium diagrams (Taylor and Sheppard, 1986). If we have sufficient knowledge in these aspects, we are able to make quantitative predictions

of the $\delta^{18}O$ changes in silicate melts during the fractional crystallization. As depicted in Figs. 7 and 8, there is a good agreement between the present calculations and the empirical estimates. In this regard, the present calculations of the oxygen isotope fractionation factors between crystals and melt (or between phenocrysts and lava) can be directly applied to natural magma systems.

For volcanic rocks, there is no subsolidus isotope exchange as plutonic rocks because of rapid quench of magma. As a result, the $\delta^{18}O$ values of quenched volcanic glasses and their coexisting phenocrysts can be used as a sensitive indicator of temperatures at which magma was solidified by use of the present calculations for the phenocrysts–lava systems. If the temperatures can be independently obtained, a calibration for oxygen isotope fractionation factors between phenocrysts and lava may be empirically carried out. The plutonic rocks cool very slowly compared to ash-flow tuffs, the subsolidus oxygen isotopic exchange between minerals down to their closure temperatures can be expected to occur, and has in fact been documented in numerous instances (e.g., Taylor, 1968; Anderson et al., 1971; Giletti, 1986). Accordingly, the measured fractionations ($\Delta^{18}O$) between the magmatic minerals from the plutonic rocks reflect lower temperature reequilibration and are greater than the measured $\Delta^{18}O$ values for the minerals from the ash-flow tuffs.

In early practices of oxygen isotope geothermometry, mineral–mineral fractionation factors were obtained by combining experimental mineral–H_2O fractionation factors (O'Neil, 1986). Discrepancies were observed when comparing the combined mineral–mineral fractionation factors with those derived from direct determinations by calcite–silicate exchange experiments (Chacko et al., 2001). Because of the isotope effects of dissolved minerals in aqueous solutions and of dissolved H_2O as hydroxyl in minerals, systematic errors were introduced when calculating the mineral–mineral fractionation factors by the simple combination of the experimental mineral–H_2O systems. Likewise, a systematic bias may also be present when calculating the phenocryst–lava fractionation factors by a direct combination of the experimental CO_2–melt fractionation factors without consideration of the isotopic effect of dissolved CO_2 in silicate melts. In this regard, the introduction of the fluid–solid interaction term has provided a resolution to the discrepancies when calculating the solid–solid fractionation factors by the combination of mineral–H_2O or CO_2–melt systems.

7. Conclusions

Oxygen isotope fractionation factors between the common magmatic rocks and water and between phenocrysts and lava are calculated in terms of the CIPW normative minerals and the normalized chemical compositions, respectively. The results from the two approaches are almost the same, and compare well with the known experimental and/or empirical calibrations. This demonstrates that oxygen isotope fractionation between rock and melt of the same chemical compositions is close to nil, and probably smaller than analytical uncertainties. Therefore, the oxygen isotopic properties of melts can be represented by the incremental values for different types of bonds in the crystalline state. Oxygen isotope index values increase with SiO_2 content from felsic to mafic to ultramafic rocks, but a linear relationship between them does not exist. The present calculations are useful to people working with such data because it provides a first approximation to oxygen isotope fractionations among minerals, melts and fluids and thus the best available reference for one's best guess should be of the fractionations.

The chemical composition of the magmatic rocks used in the present calculations is an average in the world and thus responsible for the whole-rock isotope composition of the idealized magmatic rocks. Nevertheless, the calculated fractionation factors can be widely applied to natural systems of magmatic rocks at a first approximation. The results will be more accurate if the calculations can be carried out for the chemical compositions or mineral assemblages of given magmatic rocks by a detailed analysis of modal mineralogy. It must be pointed out, however, naturally occurred melts and crystals are somewhat different from their source rocks and magmas in chemical composition. Melt–rock and crystal–magma isotope fractionations can thus arise from the chemical differentiation during melting and crystallization. The theoretical and experimental calibrations are only

applicable to the magmatic rock of corresponding compositions, provided that there is negligible oxygen isotope fractionation between the rock and melt of the same compositions.

Acknowledgements

This study was supported by funds from the Natural Science Foundation of China (No. 40033010) and the Chinese Academy of Sciences (KZCX2-107). Thanks are due to Drs. J.M. Eiler, B.E. Taylor and an anonymous reviewer for their constructive comments that helped improved this manuscript. **[RR]**

References

Anderson, A.T., Clayton, R.N., Mayeda, T.K., 1971. Isotope geothermometry of mafic magmatic rocks. J. Geol. 79, 715–729.

Appora, I., Eiler, J.M., Stolper, E.M., 2000. Experimental determination of oxygen–isotope fractionations between CO_2 vapor and soda-melilite melt. J. Conf. Abstr. 5 (2), 149–150.

Baldridge, W.S., Sharp, Z.D., Reid, K.D., 1996. Quartz-bearing basalts: oxygen isotopic evidence for crustal contamination of continental mafic rocks. Geochim. Cosmochim. Acta 60, 4765–4772.

Becker, R.H., Clayton, R.N., 1976. Oxygen isotope study of a Precambrian banded iron formation, Hamersley Range, western Australia. Geochim. Cosmochim. Acta 40, 1153–1166.

Bird, M., Longstaffe, F.J., Fyfe, W.S., 1993. Oxygen-isotope fractionation in titanium-oxide minerals at low temperatures. Geochim. Cosmochim. Acta 57, 3083–3091.

Bottinga, Y., Javoy, M., 1973. Comments on oxygen isotope geothermometry. Earth Planet. Sci. Lett. 20, 250–265.

Bowers, T.S., Taylor Jr., H.P. 1985. An integrated chemical and stable-isotope model for the origin of mid-ocean ridge hot spring systems. J. Geophys. Res. 90, 12583–12606.

Chacko, T., Mayeda, T.K., Clayton, R.N., Goldsmith, J.R., 1991. Oxygen and carbon isotope fractionation between CO_2 and calcite. Geochim. Cosmochim. Acta 55, 2867–2882.

Chacko, T., Cole, D.R., Horita, J., 2001. Equilibrium oxygen, hydrogen and carbon isotopic fractionation factors applicable to geologic systems. Rev. Mineral. Geochem. 43, 1–81.

Clayton, R.N., 1981. Isotopic thermometry. In: Newton, R.C., Navrotsky, A., Wood, B.J. (Eds.), Thermodynamics of Minerals and Melts. Springer, Berlin. pp. 85–109.

Clayton, R.N., Onuma, N., Mayeda, T.K., 1971. Oxygen isotope fractionation in Apollo 12 rocks and soils. Proc. 2nd Lunar Sci. Conf. 2, 1417–1420.

Clayton, R.N., Goldsmith, J.R., Mayeda, T.K., 1989. Oxygen isotope fractionation in quartz, albite, anorthite and calcite. Geochim. Cosmochim. Acta 53, 725–733.

Cole, D.R., Mottl, M.J., Ohmoto, H., 1987. Isotopic exchange in mineral–fluid systems: II. Oxygen and hydrogen isotopic investigation of the experimental basalt–seawater system. Geochim. Cosmochim. Acta 51, 1523–1538.

Cole, D.R., Ohmoto, H., Jacobs, G.K., 1992. Isotopic exchange in mineral–fluid systems: III. Rates and mechanisms of oxygen isotope exchange in the system granite–$H_2O\pm NaCl\pm KCl$ at hydrothermal conditions. Geochim. Cosmochim. Acta 56, 445–466.

Eiler, J.M., 2001. Oxygen isotope variations of basaltic lavas and upper mantle rocks. Rev. Mineral. Geochem. 43, 319–364.

Eiler, J.M., Farley, K.A., Valley, J.W., Stolper, E.M., Hauri, E., Craig, H., 1995. Oxygen isotope evidence against bulk recycled sediment in the source of Pitcairn Island lavas. Nature 377, 138–141.

Eiler, J.M., Farley, K.A., Valley, J.W., Hofmann, A.W., Stolper, E.M., 1996a. Oxygen isotope constraints on the sources of Hawaiian volcanism. Earth Planet. Sci. Lett. 144, 453–468.

Eiler, J.M., Stolper, E.M., Valley, J.W., 1996b. Oxygen isotope ratios in olivine from the Hawaiian scientific drilling project. J. Geophys. Res. 101, 11807–11813.

Eiler, J.M., Farley, K.A., Valley, J.W., Hauri, E., Craig, H., Hart, S.R., Stolper, E.M., 1997. Oxygen isotope variations in ocean island basalt phenocrysts. Geochim. Cosmochim. Acta 61, 2281–2293.

Eiler, J.M., Crawford, A., Elliott, T., Farley, K.A., Valley, J.W., Stolper, E.M., 2000. Oxygen isotope geochemistry of oceanic-arc lavas. J. Petrol. 41, 229–256.

Epstein, S., Taylor Jr., H.P., 1971. $^{18}O/^{16}O$, $^{30}Si/^{28}Si$, D/H, and $^{13}C/^{12}C$ ratios in lunar samples. Proc. 2nd Lunar Sci. Conf. 2, 1421–1441.

Fu, B., Zheng, Y.-F., Wang, Z.-R., Xiao, Y.-L., Gong, B., Li, S.-G., 1999. Oxygen and hydrogen isotope geochemistry of gneisses associated with ultrahigh pressure eclogites at Shuanghe in the Dabie Mountains. Contrib. Mineral. Petrol. 134, 52–66.

Ganor, J., Matthews, A., Schliestedt, M., 1994. Post-metamorphic low $\delta^{13}C$ calcite in the Cycladic complex (Greece) and their implications for modeling fluid infiltration processes using carbon isotope compositions. Eur. J. Mineral. 6, 365–379.

Garlick, G.D., 1966. Oxygen isotope fractionation in magmatic rocks. Earth Planet. Sci. Lett. 1, 361–368.

Giletti, B.J., 1986. Diffusion effect on oxygen isotope temperatures of slowly cooled magmatic and metamorphic rocks. Earth Planet. Sci. Lett. 77, 218–228.

Harris, C., Smith, H.S., le Roex, A.P., 2000. Oxygen isotope composition of phenocrysts from Tristan da Cunha and Gough Island lavas: variation with fractional crystallization and evidence for assimilation. Contrib. Mineral. Petrol. 138, 164–175.

Hattori, K., Halas, S., 1982. Calculation of oxygen isotope fractionation between uranium dioxide, uranium trioxide and water. Geochim. Cosmochim. Acta 46, 1863–1868.

Kalamarides, R.I., 1984. Kiglapait geochemistry VI: Oxygen isotopes. Geochim. Cosmochim. Acta 48, 1827–1836.

Kalamarides, R.I., 1986. High-temperature oxygen isotope fractionation among the phases of the Kiglapait intrusion, Labarador, Canada. Chem. Geol. 58, 303–310.

Kieffer, S.W., 1982. Thermodynamics and lattice vibrations of min-

erals: 5. Applications to phase equilibria, isotope fractionation, and high-pressure thermodynamic properties. Rev. Geophys. Space Phys. 20, 827–849.

Kyser, T.K., O'Neil, J.R., Carmichael, I.S.E., 1981. Oxygen isotope thermometry of basic lavas and mantle nodules. Contrib. Mineral. Petrol. 77, 11–23.

Kyser, T.K., O'Neil, J.R., Carmichael, I.S.E., 1982. Genetic relations among basic lavas and ultramafic nodules: evidence from oxygen isotope compositions. Contrib. Mineral. Petrol. 81, 88–102.

Le Maitre, R.W., 1976. The chemical variability of some common magmatic rocks. J. Petrol. 17, 589–637.

Macpherson, C.G., Mattey, D.P., 1997. Oxygen isotope variations in Lau Basin lavas. Chem. Geol. 144, 177–194.

Matsuhisa, Y., 1979. Oxygen isotopic compositions of volcanic rocks from the East Japan Island Arcs and their bearing on petrogenesis. J. Volcanol. Geotherm. Res. 5, 271–296.

Matthews, A., Palin, J.M., Epstein, S., Stolper, E.M., 1994. Experimental study of $^{18}O/^{16}O$ partitioning between crystalline albite, albitic glass, and CO_2 gas. Geochim. Cosmochim. Acta 58, 5255–5266.

Matthews, A., Stolper, E.M., Eiler, J.M., Epstein, S., 1998. Oxygen isotope fractionation among melts, minerals and rocks. Mineral. Mag. 62A, 971–972.

Mottl, M.J., 1983. Metabasalts, axial hot springs, and the structure of hydrothermal systems at mid-ocean ridges. Bull. Geol. Soc. Am. 94, 161–180.

Muehlenbachs, K., Byerly, G., 1982. ^{18}O-enrichment of silicic magmas caused by crystal fractionation at the Galapagos spreading center. Contrib. Mineral. Petrol. 79, 76–79.

Muehlenbachs, K., Clayton, R.N., 1972. Oxygen isotope studies of fresh and weathered submarine basalts. Can. J. Sci. 9, 172–184.

Muehlenbachs, K., Kushiro, I., 1974. Oxygen isotope exchange and equilibrium of silicates with CO_2 or O_2. Carnegie Inst. Washington, Year Book 73, 232–236.

O'Neil, J.R., 1986. Theoretical and experimental aspects of isotopic fractionation. Rev. Miner. 16, 1–40.

O'Neil, J.R., Adami, L.H., 1970. Oxygen isotope analyses of selected Apollo II materials. Proc. Apollo II Lunar Sci. Conf. 2, 1425–1427.

Palin, J.M., Epstein, S., Stolper, E.M., 1996. Oxygen isotope partitioning between rhyolitic glass/melt and CO_2: an experimental study at 500–950 °C and 1 bar. Geochim. Cosmochim. Acta 60, 1963–1973.

Polyakov, V.B., Mineev, S.D., 2000. The use of Moessbauer spectroscopic data in stable isotope geochemistry. Geochim. Cosmochim. Acta 64, 849–865.

Reed, M.H., 1983. Seawater–basalt reaction and the origin of greenstones and related ore deposits. Econ. Geol. 78, 466–485.

Rosenbaum, J.M., Mattey, D., 1995. Equilibrium garnet–calcite oxygen isotope fractionation. Geochim. Cosmochim. Acta 59, 2839–2842.

Schliestedt, M., Matthews, A., 1987. Transformation of blueschist to greenschist facies rocks as a consequence of fluid infiltration, Sifnos (Cyclades), Greece. Contrib. Mineral. Petrol. 97, 237–250.

Schütze, H., 1980. Der Isotopenindex-eine Inkrementenmethode zur näherungsweise Berechnung von Isotopenaustauschgleichgewichten zwischen kristallinen Substanzen. Chem. Erde 39, 321–334.

Sheppard, S.M.F., Harris, C., 1985. Hydrogen and oxygen isotope geochemistry of Ascension island lavas and granites: variation with crystal fractionation and interaction with sea water. Contrib. Mineral. Petrol. 91, 74–81.

Stolper, E., Epstein, S., 1991. An experimental study of oxygen isotope partitioning between silica glass and CO_2 vapor. In: Taylor Jr., H.P., O'Neil, J.R., Kaplan, I. (Eds.), Stable Isotope Geochemistry: A Tribute to Samuel Epstein. Geochem. Soc. Spec. Publ., vol. 3, pp. 35–51.

Taylor Jr., H.P. 1968. The oxygen isotope geochemistry of magmatic rocks. Contrib. Mineral. Petrol. 19, 1–21.

Taylor Jr., H.P., 1971. Oxygen isotope evidence for large-scale interaction between meteoric ground waters and Tertiary granodiorite intrusions, western Cascade Range, Oregon. J. Geophys. Res. 76, 7855–7874.

Taylor Jr., H.P., 1974. The application of oxygen and hydrogen isotope studies to problems of hydrothermal alteration and ore deposition. Econ. Geol. 69, 843–883.

Taylor Jr., H.P., 1988. Oxygen, hydrogen, and strontium isotope constraints on the origin of granites. Trans. R. Soc. Edinb. Earth Sci. 79, 317–338.

Taylor Jr., H.P., Epstein, S. 1962. Relationships between $^{18}O/^{16}O$ ratios in coexisting minerals of magmatic and metamorphic rocks: Part. I. Principles and experimental results. Geol. Soc. Amer. Bull. 73, 461–480.

Taylor Jr., H.P., Epstein, S. 1970. Oxygen and silicon isotope ratios of lunar rock 12013. Earth Planet. Sci. Lett. 9, 208–210.

Taylor Jr., H.P., Sheppard, S.M.F. 1986. Magmatic rocks: I. Processes of isotopic fractionation and isotope systematics. Rev. Miner. 16, 227–271.

Wolery, T.J., 1978. Some chemical aspects of hydrothermal process at mid-ocean ridges—A theoretical study: I. Basalt–seawater reaction and chemical cycling between the oceanic crust and the oceans; II. Calculation of chemical equilibrium between aqueous solutions and minerals. PhD Thesis, Northwestern Univ., Evanston, Ill.

Wolery, T.J., 1979. Calculation of chemical equilibrium between aqueous solutions and minerals: The EQ3/6 software package. Rep. UCRL52658, Lawrence Livermore Natl. Lab., Livermore, CA.

Wolery, T.J., 1983. EQ3NR, a computer program for geochemical aqueous speciation-solubility calculations. Rep. UCRL 5, Distrib. Category UC-70, Lawrence Livermore Natl. Lab., Livermore, CA.

Xiao, Y.-L., Hoefs, J., van den Kerkhof, A.M., Fiebig, J., Zheng, Y.-F., 2002. Fluid history of UHP metamorphism in Dabieshan, China: a fluid inclusion and oxygen isotope study on the coesite-bearing eclogite from Bixiling. Contrib. Mineral. Petrol. 139, 1–16.

Xu, B.-L., Zheng, Y.-F., 1998. Experimental studies of oxygen and hydrogen isotope fractionations between precipitated brucite and water at low temperatures. Geochim. Cosmochim. Acta 63, 2009–2018.

Zhang, L.-G., Liu, J.-X., Chen, Z.-S., Zhou, H.-B., 1994. Experi-

mental investigations of oxygen isotope fractionation in cassiterite and wolframite. Econ. Geol. 89, 150–157.

Zheng, Y.-F., 1991. Calculation of oxygen isotope fractionation in metal oxides. Geochim. Cosmochim. Acta 55, 2299–2307.

Zheng, Y.-F., 1992. Oxygen isotope fractionation in wolframite. Eur. J. Mineral. 4, 1331–1335.

Zheng, Y.-F., 1993a. Calculation of oxygen isotope fractionation in anhydrous silicate minerals. Geochim. Cosmochim. Acta 57, 1079–1091.

Zheng, Y.-F., 1993b. Calculation of oxygen isotope fractionation in hydroxyl-bearing silicates. Earth Planet. Sci. Lett. 120, 247–263.

Zheng, Y.-F., 1995. Oxygen isotope fractionation in magnetites: structural effect and oxygen inheritance. Chem. Geol. 121, 309–316.

Zheng, Y.-F., 1996. Oxygen isotope fractionations involving apatites: application to palaeotemperature determination. Chem. Geol. 127, 177–187.

Zheng, Y.-F., 1997. Prediction of high-temperature oxygen isotope fractionation factors between mantle minerals. Phys. Chem. Miner. 24, 356–364.

Zheng, Y.-F., 1998. Oxygen isotope fractionation between hydroxide minerals and water. Phys. Chem. Miner. 25, 213–221.

Zheng, Y.-F., 1999a. Oxygen isotope fractionation in carbonate and sulfate minerals. Geochem. J. 33, 109–126.

Zheng, Y.-F., 1999b. On calculation of oxygen isotope fractionation in minerals. Episodes 22, 99–106.

Zheng, Y.-F., Fu, B., Li, Y.-L., Xiao, Y.-L., Li, S.-G., 1998. Oxygen and hydrogen isotope geochemistry of ultrahigh pressure eclogites from the Dabie Mountains and the Sulu terrane. Earth Planet. Sci. Lett. 155, 113–129.

Zheng, Y.-F., Fu, B., Xiao, Y.-L., Li, Y.-L., Gong, B., 1999. Hydrogen and oxygen isotope evidence for fluid–rock interactions in the stages of pre- and post-UHP metamorphism in the Dabie Mountains. Lithos 46, 677–693.

Zheng, Y.-F., Fu, B., Li, Y.-L., Wei, C.-S., Zhou, J.-B., 2001. Oxygen isotope composition of granulites from Dabieshan in eastern China and its implications for geodynamics of Yangtze plate subduction. Phys. Chem. Earth, Part A 26, 673–684.

Zheng, Y.-F., Wang, Z.-R., Li, S.-G., Zhao, Z.-F., 2002. Oxygen isotope equilibrium between eclogite minerals and its constraints on mineral Sm–Nd chronometer. Geochim. Cosmochim. Acta 66, 625–634.

Zhou, G.-T., Zheng, Y.-F., 2002. Kinetic mechanism of oxygen isotope disequilibrium in precipitated witherite and aragonite at low temperatures: an experimental study. Geochim. Cosmochim. Acta 66, 63–71.